Energy for Sustainable Development 26 (2015) 1–13

Contents lists available at ScienceDirect

Energy for Sustainable Development

Modeling of household biomass cookstoves: A review

Nordica A. MacCarty, Kenneth M. Bryden [1]

Department of Mechanical Engineering, Iowa State University, Ames, IA 50011, USA

ARTICLE INFO

Article history:
Received 26 July 2014
Revised 2 February 2015
Accepted 3 February 2015
Available online xxxx

Keywords:
Cookstoves
Biomass
Computational modeling
Heat transfer
Combustion
Review

ABSTRACT

This article reviews the cookstove modeling literature for one- to three-burner natural draft, wood-fired cookstoves fueled with solid unprocessed biomass ranging in size from 1 to 20 cm and operated by an individual in a residential setting. These household cookstove models are organized around the three major zones of the cookstove system: the fuel bed, the gas phase reaction zone, and the heat transfer zone. Today's household biomass cookstove models are coupled steady-state models with simplified algebraic relationships for the packed bed; computational fluid dynamics with a four-equation set global reaction scheme for CO_2, CO, H_2, H_2O, and hydrocarbons in the gas phase reaction zone; and generic correlations or computational fluid dynamics models in the heat transfer zone. The current models do not address the production of particulate or other harmful emissions or the effects of fuel tending, varying fuel, or transient operations.

Introduction

This paper reviews the current state of numerical modeling of the small biomass cookstoves used to meet the household energy needs of more than 2.4 billion people. Specifically, this article focuses on one- to three-burner biomass cookstoves fueled with solid unprocessed biomass ranging in size from 1 to 20 cm and operated by an individual in a residential setting. Although called cookstoves, depending on local custom and need, the primary uses of these stoves include heating water for washing, cooking meals, steeping tea, making medicines, and other household tasks (Johnson and Bryden, 2012). These types of stoves account for the majority of cookstove designs in use in the developing world today (Jetter et al., 2012; MacCarty et al., 2010). Although in some cases the issues are similar, this article does not address charcoal or coal stoves, forced draft stoves, gasifier stoves, pulverized fuel stoves, institutional scale stoves, or stoves used for space heating. Nor does this article address the issues associated with fuel processing and fuel pellets.

More than 2.4 billion people use solid biomass fuels for household cooking and heating in open fires and simple stoves (International Energy Agency (IEA), 2010). The users of these cookstoves live almost entirely in the developing world, and the individual, community, and global impacts of these household biomass cookstoves are significant. It has been estimated that indoor air pollution from solid fuel use is responsible for nearly 4 million deaths annually and accounts for approximately 4% of the burden of disease in developing countries (Lim et al., 2012; World Health Organization (WHO), 2002). The fine particulate matter, carbon monoxide, polycyclic aromatic hydrocarbons, and other emissions due to incomplete combustion within typical kitchens contribute to acute lower respiratory infections, pneumonia, and chronic obstructive lung disease; as well as adverse pregnancy outcomes and cataracts (World Health Organization (WHO), 2002; Legros et al., 2009; Bruce et al., 2006; Rehfuess, 2006). In addition, the use of biomass fuel for cooking and heating is a significant source of global black carbon emissions, which is one source of climate change (Bond et al., 2013).

Recognizing these individual, community, and global impacts, a number of groups have focused on the research and development of improved household biomass cookstoves. However, few of these efforts have focused on developing the numerical models needed for the design of cookstoves. In the past 30 years more than 500 journal articles have examined various aspects of biomass cookstoves; however, fewer than 30 of these journal articles have addressed numerical modeling of the heat transfer and combustion processes in traditional household biomass cookstoves. Because of this, today the design of these cookstoves is primarily based on experience and rules of thumb.

Background

A traditional biomass cookstove consists of the air intake and transport system, a bed of fuel, a gas phase combustion zone, and a cookpot. There are three primary types of traditional household biomass cookstoves based on the treatment of the combustion chamber. These are

E-mail address: kmbryden@iastate.edu (K.M. Bryden).
[1] 1620 Howe Hall, Iowa State University, Ames, IA 50011, USA. Tel.: +1 515 294 3891; fax: +1 515 294 3261.

http://dx.doi.org/10.1016/j.esd.2015.02.001
0973-0826/

1. Open cooking fires—these are traditional cooking fires in which a cookpot is held atop three stones or other similar support (Fig. 1a). The airflow is uncontrolled and the air is entrained in the system due to buoyancy. Generally a fire grate is not included.
2. Shielded-fire cookstove—these stoves are often referred to as improved stoves and marketed under a number of names. These devices range from a simple shield of metal or clay around the combustion space to more complex devices with inlets for the directed control of primary and secondary air (Fig. 1b). Some include electrically powered fans to control the air. In some cases a narrow channel is created around the cookpot to improve heat transfer from the combustion gases to the cookpot. There may or may not be a fire grate provided.
3. Enclosed-fire cookstoves with chimneys—these stoves are similar to stoves used for space heating but have high temperature cooking surfaces (Fig. 1c). The fire is fully enclosed within the combustion chamber. The fuel entrance may be open and permit airflow into the system. Alternately, there may be a tightly sealed fuel door and separate controls for airflow into the stove. Gases leave the combustion chamber and travel along channels underneath exposed cookpot bottoms or a large sealed plate or griddle on which pots are heated or food is directly cooked. The combustion gases then exit to the chimney and are exhausted outside of the kitchen.

The basic operation of all three types of stoves is similar. They are fueled with wood or biomaterials (e.g., dung cake or crop residues). It should be noted that there are very few models of cookstoves fired with biomaterials other than wood, and all the models included in this review are based on wood-fired cookstoves. The wood fuels that have been modeled range in size from small twigs to large unsplit branches. The as-received fuel moisture varies in moisture content from 5% to greater than 50% depending on the season, storage availability, harvest method, and curing time (Ragland and Bryden, 2011). Due to limited control of primary and secondary airflow, there is often high excess air resulting in low combustion gas temperatures, short transit times, and incomplete combustion. The challenge for designers of these devices is to create a user-friendly cooking appliance that can utilize a wide array of fuel types, sizes, and moisture contents while maintaining high heat, good turndown, high overall efficiency and low emissions.

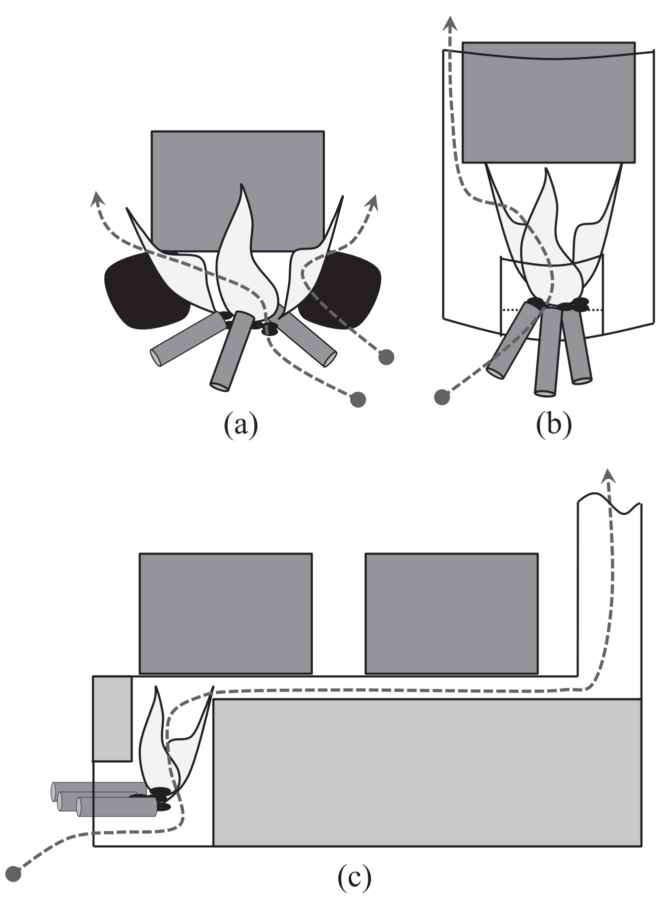

Fig. 1. Types of cookstoves: (a) open cooking fire, (b) shielded-fire cookstove, (c) enclosed fire with chimney.

Cookstove models

Fig. 2 provides a schematic of a small biomass cookstove of the type used in nearly all numerical models. In general the goal of cookstove modeling has been to improve heat transfer efficiency of the cookstove system by examining the relationships between the combustion rate, excess air, geometry, and heat transfer. In all cases zonal models have been used to describe and couple the processes occurring within the three major zones of the cookstove system—the reacting fuel bed zone, the gas phase combustion zone, and the heat transfer zone around the cookpot.

Table 1 provides a summary of various cookstove modeling efforts over the past 30+ years. To understand past modeling work and the current state of progress towards a complete stove model, it is helpful to divide Table 1 into five groups of stove models. Four of these groups model the entire cookstove and are differentiated based on the coupling between the zones and how the gas phase reaction zone is modeled. The final group of models consists of models that address only a single aspect of cookstove design (e.g., heat transfer). The five groups are

1. Uncoupled models with no explicit gas phase combustion—these models do not include coupling between various zones of the stove in which results from one zone are used as inputs to a subsequent zone (De Lepeleire et al., 1981; Verhaart, 1982; Prasad et al., 1985; Baldwin, 1987). Rather, the boundary condition inputs (e.g., temperature and velocity) to each zone were assumed separately.
2. Coupled models with no explicit gas phase combustion—the Woodburning Stove Group at Eindhoven University over a period of years developed a set of models that couple solid phase combustion in the fuel bed together with buoyant flow in the flame zone to predict the heat transfer (Bussmann and Prasad, 1982; Bussmann et al., 1983; De Lepeleire and Christiaens, 1983;

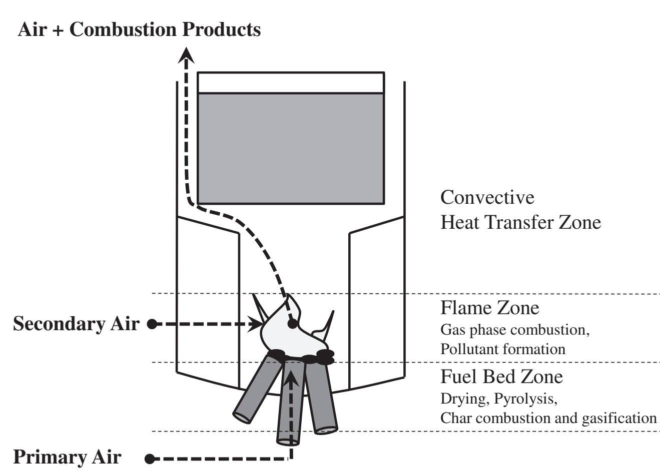

Fig. 2. Processes within a cookstove.

Table 1
A chronological summary of household biomass cookstove modeling efforts.

Model	Model type[a]	Stove type[b]	Model characteristics	Validation
De Lepeleire et al. (1981)	1	EN	Description—combustion stoichiometry used to determine combustion chamber and primary/secondary air inlet dimensions for given firepower and excess air Packed bed model—no separate packed bed model Gas phase combustion model—no separate gas phase combustion model Heat transfer model—no separate heat transfer model	None
Verhaart (1982)	1	EN	Description—empirical velocity of fire penetration used to determine whether heat supplied by char and volatile combustion can sustain a constant firepower Packed bed model—no separate packed bed model Gas phase combustion model—no separate gas phase combustion model Heat transfer model—no separate heat transfer model	None
Bussmann and Prasad (1982), Bussmann et al. (1983)	2	OF	Description—coupled zonal model to predict temperature, plume width, and velocity for varying firepower, excess air, and volatile fraction Packed bed model—conservation of energy for a control volume with given firepower and volatile fraction Gas phase combustion model—differential conservation equations including reacting flow with air entrainment Heat transfer model—local convective heat transfer correlations for bottom and sides of pot, blackbody radiation with nonparticipating media	Quantitative and qualitative experimental
De Lepeleire and Christiaens (1983)	2	EN	Description—coupled flow and heat transfer analysis to investigate effects of several geometrical variables Packed bed model—given temperature Gas phase combustion model—no separate gas phase combustion model Heat transfer model—convective heat transfer correlation for short duct with laminar flow	None
Prasad et al. (1985)	1	SF	Description—transient wall loss analysis for three body materials Packed bed model—no separate packed bed model Gas phase combustion model—no separate gas phase combustion model Heat transfer model—no separate heat transfer model	None
Bussmann and Prasad (1986)	2	SF	Description—coupled zonal model to predict efficiency for parametric variation of geometric variables Packed bed model—same as Bussmann et al. (1983) Gas phase combustion model—heat addition of complete combustion, non-reacting flow Heat transfer model—adiabatic wall, local convective heat transfer correlations for bottom and sides of pot, blackbody radiation with nonparticipating media	Experimental
Baldwin (1987)	1	SF	Description—discussion and uncoupled models of steady-state and transient combustion and heat transfer processes to investigate effects of design variables Packed bed model—simplified pyrolysis and 2-step char burning models presented Gas phase combustion model—assumed temperature and velocity input to heat transfer zone Heat transfer model—investigated effects of material and geometry on wall losses via thermal resistance analog, global convective heat transfer for the pot side, blackbody radiation using fuel bed reduction factor of 0.5	Qualitative experimental
Date (1988)	2	SF	Description—coupled zonal model to predict efficiency for parametric variation of geometric variables Packed bed model—time-averaged and temperature dependent char burning and volatile evolution for various wood diameter Gas phase combustion model—heat addition of complete combustion, reactions added in (Shah and Date, 2011) Heat transfer model—wall losses as thermal resistance analog, global convective heat transfer correlations from the literature, radiation with participating media as a function of beam length	Experimental
Kumar et al. (1990)	2	EN	Description—coupled zonal model to predict heat transfer and flue gas composition for varied firepower Packed bed model—conservation of energy for a control volume given constant firepower, excess air, and mass of char remaining, no radiative losses Gas phase combustion model—conservation of energy for a control volume in terms of specific heat of products of complete combustion Heat transfer model—six well-stirred reactors with convective heat transfer correlations from literature, cumulative conductive wall losses, and radiation as a function of CO_2, H_2O and beam length	Experimental
Schutte et al. (1991)	5	E	Description—presented discussion for predicting flue gas composition in downdraft and traditional combustion with constant firepower Packed bed model—no separate packed bed model Gas phase combustion model—reacting flow using reaction rates from literature including C, CO, CO_2 and H_2O	Experimental

(continued on next page)

Table 1 (*continued*)

Model	Model type[a]	Stove type[b]	Model characteristics	Validation
Weerasinghe and Kumara (2003)	4	SF	Heat transfer model—no separate heat transfer model Description—coupled CFD model of flaming mode of combustion and heat transfer to determine optimal height Packed bed model—no separate packed bed model Gas phase combustion model—reaction rate of fuel combustion according to dissipation rates Heat transfer model—CFD analysis	Heat transfer experimental
Bryden et al., 2003	5	EN	Description—CFD simulation to optimize baffle placement with empirical inlet conditions Packed bed model—no separate packed bed model Gas phase combustion model—no separate gas phase combustion model Heat transfer model—CFD analysis to optimize heat transfer through griddle with inputs to heat transfer zone determined experimentally	Experimental
Burnham-Slipper et al. (2007a,b), Burnham-Slipper (2008)	4	SF	Description—CFD, analytical, and experimental studies of combustion and heat transfer to a flat plate for design optimization. Packed bed model—simplified steady-state CFD model developed for a fixed crib of fuel, with pyrolysis limited by heat conduction through char and char combustion limited by oxygen diffusion Gas phase combustion model—CFD model using species transport limited by turbulent mixing Heat transfer model—CFD analysis of impinging jet, radiation as weighted sum of gray gases	Experimental and from literature
Wohlgemuth et al. (2010)	5	SF	Description—CFD analysis of heat transfer for varying pot shield dimension and material using empirical inlet conditions Packed bed model—no separate packed bed model Gas phase combustion model—no separate gas phase combustion model Heat transfer model—CFD analysis of heat transfer within pot shield, radiation as gray gases with no scattering and tuned absorption coefficient with inputs to heat transfer zone determined experimentally from detuned gas burner	Experimental used to tune unknown parameters
Gupta and Mittal (2010a,b)	4	SF	Description—CFD simulation of flow and heat transfer for varying operating and geometric variables Packed bed model—assumed uniform 40% of heat release, permeability expressed through Karman–Cozeny relationship Gas phase combustion model—assumed uniform 60% of heat release Heat transfer model—CFD analysis	From literature
Agenbroad et al. (2011a,b)	5	SF	Description—analytical model to predict bulk flow rate, temperature, and excess air as a function of firepower and geometry for an adiabatic combustion chamber with no pot Packed bed model—no separate packed bed model Gas phase combustion model—no separate gas phase combustion model Heat transfer model—no separate heat transfer model	Experimental
Shah and Date (2011)	3	SF	Description—coupled zonal model to predict efficiency and combustion products for parametric variation of geometric variables Packed bed model—taken from Date (1988) Gas phase combustion model—4-step Hautmann quasi-global reaction treating stove regions as well-stirred reactors Heat transfer model—taken from Date (1988)	From literature
Joshi et al. (2012)	5	SF	Description—CFD analysis of flow and temperature in pot shield to determine optimal gap Packed bed model—no separate packed bed model Gas phase combustion model—no separate gas phase combustion model Heat transfer model—CFD analysis of heat transfer within pot shield with inputs determined experimentally from LPG burner	Experimental

[a] Model types: 1. Uncoupled with no explicit gas phase combustion; 2. Coupled with no explicit gas phase combustion; 3. Coupled with explicit gas phase combustion; 4. Coupled with CFD; 5. Single aspect.
[b] Stove types: OF—open fire; SF—shielded fire; EN—enclosed stove.

Bussmann and Prasad, 1986). The intention of these and other models was to understand the effects of geometry on the airflow and efficiency of open fires and shielded-fire stoves (Date, 1988; Kumar et al., 1990).

3. Coupled models with explicit gas phase combustion—this model couples the three major zones and includes the evolution of volatiles along the flow path using an explicit model of the gas phase reactions (Shah and Date, 2011).
4. Coupled models that utilize computational fluid dynamics (CFD)—in these studies CFD is used to model the gas phase reaction zone including turbulence, heat transfer with radiation, and/or volatile evolution and to provide greater detail of processes within the heat transfer zone (Weerasinghe and Kumara, 2003; Burnham-Slipper et al., 2007a,b; Burnham-Slipper, 2008; Gupta and Mittal, 2010a,b).
5. Single aspect models—several models have been developed that address one or two cooking stove design questions without explicitly modeling all three zones (Schutte et al., 1991; Bryden et al., 2003; Burnham-Slipper et al., 2007a; Wohlgemuth et al., 2010; Agenbroad et al., 2011a,b; Joshi et al., 2012).

As a general observation, each of these modeling efforts was developed independently with limited reference to earlier or concurrent cookstove modeling efforts. This appears to have occurred largely due to the lack of explicit outlets for scholarly publication of cookstove modeling efforts and conference venues for collaboration and discussion.

Uncoupled models with no explicit gas phase combustion

Baldwin (1987) developed two models to examine the effects of geometry and material on the thermal performance of a shielded-fire biomass cookstove. These models focused on heat loss through the stove wall and the heat transfer zone around the cookpot. The first model examined the steady-state heat loss through the stove wall as a function of the stove body material and the geometry of the stove. The second model provided a detailed analysis of heat transfer to the sides of the cookpot. Although pyrolysis and combustion of solid biomass fuels in the fuel bed are discussed, no specific model for the fuel bed was developed. Rather, a simplified pyrolysis and char combustion model for a single biomass particle is presented, and the results of the single particle model are discussed in the context of a reacting packed bed of wood. The gas phase combustion zone was not modeled. Instead, it was assumed that the gas phase combustion zone was at a uniform gas temperature of 700 K. In addition the temperature at the top of the fuel bed is assumed to be 1000 K.

Using these assumptions, the heat transfer through a planar stove wall with convection heat transfer on both sides of the wall is

$$q''_{wall} = \frac{T_g - T_{amb}}{\frac{1}{\tilde{h}_{wall,int,tot}} + \frac{W_{wall}}{\tilde{k}_{wall}} + \frac{1}{\tilde{h}_{wall,ext}}}. \tag{1}$$

The related equations for cylindrical and spherical geometries are also compared. The heat transfer coefficient on the interior wall was modified to include radiation heat transfer from the fuel bed and cookpot bottom to the wall of the stove assuming that the fuel bed and the cookpot bottom are parallel circular disks of equal size.

$$\tilde{h}_{wall,\,int,tot} = \tilde{h}_{wall,\,int} + \sigma\varepsilon_{bed}A_{bed}F_{bed-wall}\left[\frac{\beta T_{bed}^4 + T_{pot}^4 - 2T_{int}^4}{T_g - T_{int}}\right] \tag{2}$$

where $F_{bed\text{-}wall}$ is the view factor between the bed and the wall. To account for the fire not covering the entire area of the fuel bed, the effective size of the fire was reduced by a factor, β, where

$$\beta = 0.5.$$

The convective heat transfer coefficient was generally assumed to be

$$\tilde{h}_{int} = 10\ \mathrm{W/m^2 \cdot K}$$

To account for cases where the temperature difference between the exterior of the stove and the ambient temperature is small, the convection heat transfer coefficient of the outer wall of the stove was assumed to be the greater of the natural convection heat transfer coefficient for a vertical heated plate

$$\tilde{h}_{wall,ext} = 1.42\left[\frac{T_{ext} - T_{amb}}{H_{stove}}\right]^{0.25}\ \mathrm{W/m^2 \cdot K} \tag{3}$$

or a fixed value

$$\tilde{h}_{wall,ext} = 5\ \mathrm{W/m^2 \cdot K}.$$

The conduction term W_{wall}/k_{wall} in Eq. (1) was expanded to account for various materials such as insulation using a thermal resistance analog (Incropera et al., 2007). The effect of a double metal wall with dead air space was calculated by applying the above equations to each wall separately with the effective convective heat transfer coefficient for the interior dead air space between walls at temperature T_1 and T_2 (Holman, 2009).

$$\tilde{h}_{airspace} = 3.93\delta^{-0.1389}H_c{}^{-0.111}\left[\frac{(T_1 - T_2)^{0.25}}{(T_1 - T_2)^{0.317}}\right]\ \mathrm{W/m^2 \cdot K} \tag{4}$$

In the heat transfer zone, heat transfer to the cookpot was divided into the cookpot bottom and the shielded cookpot side. Radiation heat transfer and convection heat transfer to the cookpot bottom were assumed to be 20% of the energy released from combustion of the fuel. Convective heat transfer to the shielded cookpot side was determined by a uniform, one-dimensional discretization along the vertical axis of the channel between the cookpot side and the cookpot shield and performing an integral energy balance. This is

$$\Delta z\left(\tilde{h}_{side}\right)(T_i - T_{side}) + \Delta z\left(\tilde{h}_{sh}\right)(T_i - T_{sh}) = \Delta r\left(V_i\rho_i c_{p(i)}\right)(T_{i+1} - T_i) \tag{5}$$

for segment $i = 1$ to n. The inlet temperature to the channel was assumed to be

$$T_1 = 900\ \mathrm{K}$$

where heat transfer coefficients were calculated using empirical values of the Nusselt number for various geometry and flow schemes for fully developed laminar flow, with a baseline Nusselt number of 4.861 for the sides of the cookpot and zero for the Nusselt number inside the insulated cookpot shield (i.e., no heat transfer through the insulated cookpot shield). These and other model parameters were varied to verify the robustness of the model. The velocity was found by balancing the buoyancy due to the density difference of the combustion products and the friction loss in the channel for each segment. The combustion product gases were assumed to have the same properties and density as air and were a function of temperature. The model was run with baseline parameters of $\mathrm{Nu}_{pot} = 4.861$ and $\mathrm{Nu}_{wall} = 0$ (varied up to 4.86), and the cookpot and shield temperatures were assumed to be constant at 373 K. As shown in Table 2, as the width of the gap between the stove and the shield, W_{gap}, becomes smaller, the rate of heat transfer to the stove wall increases; however, as the width of the gap between the stove and the shield becomes smaller, the resistance to the airflow increases, decreasing the airflow through the stove, which decreases the firepower of the stove. As a result, both the thermal efficiency and the firepower of the stove are very sensitive to the width of the gap between the stove and the shield. In contrast, because most of the heat transfer from the hot gases to the cookpot occurs at the beginning of the channel, the overall heat transfer to the stove wall (and the efficiency and fire power of the stove) is much less sensitive to increases in the channel length. In spite of this, increases in channel length can be used in part to offset the increases in gap width needed to maintain the firepower of the stove. These results are similar to those of Bussmann and Prasad (Bussmann and Prasad, 1986) who showed that narrower gaps and longer cookpot shields increase thermal efficiency. A simple analysis of radiation heat transfer from the fuel bed to the cookpot bottom was also performed by Baldwin. This analysis revealed that lowering the height of the cookpot, H_c, or increasing the cookpot diameter, D_{pot}, generally increases the thermal efficiency. It

Table 2
Stove efficiency as a function of channel length and gap between the cookpot and the shield (Baldwin, 1987).

		Length (cm)			
		5	10	15	20
Gap (mm)	6	38%	45%	47%	48%
	8	30%	35%	38%	42%
	10	25%	28%	32%	34%
	12	23%	25%	27%	29%
	14	22%	23%	24%	25%

was also noted that higher wall temperatures increase thermal efficiency.

Although the Baldwin models were primarily steady state, transient heat loss through the combustion chamber wall construction schemes was considered. In this case the transient heat conduction equation

$$\rho c_p \forall \frac{\partial T}{\partial t} = \widetilde{h}_{int} A_{int}(T_{int} - T) - \widetilde{h}_{ext} A_{ext}(T - T_{ext}) \tag{6}$$

was numerically solved for the combustion chamber using the assumptions developed for the steady-state case for various wall materials, construction types, thicknesses, and emissivities. The conclusions are similar to those of Prasad et al. (1985) and are that a lightweight metal wall with 1 cm of insulation or dead air space resulted in the lowest heat losses through the cylindrical combustion chamber wall, followed by fired clay, bare metal, and a massive stove wall. The massive stove began to lose less heat than the bare metal after about 90 min of operation.

Coupled models with no explicit gas phase combustion

Throughout the 1980s a group of researchers at Eindhoven University worked to understand household biomass cookstoves. Initially these efforts focused on one or more aspects of household biomass cookstoves. This included developing a simplified set of equations for sizing the combustion chamber and air inlets for enclosed-fire cookstoves as a function of the combustion stoichiometry (De Lepeleire et al., 1981) and developing an empirical relationship between the heat release rate of the char to the heat release rate of the volatiles for various sizes and shapes of wood (Verhaart, 1982). Bussmann and Prasad developed a detailed model of the gas phase region of an open fire above a fixed bed of fuel with no cookpot (Bussmann and Prasad, 1982). Using differential conservation equations for mass, momentum, and energy, the gas phase combustion zone was modeled as a steady-state, two-dimensional axisymmetric cylinder in which the pyrolysis products from the fuel bed form a rising plume that entrains the secondary air. As the plume rises, the diameter of the plume shrinks and the velocity increases. Gas velocities and temperature within the plume were assumed to be a function of height but not diameter. Gas velocity and temperature outside the plume were assumed to be zero and ambient, respectively. Other model assumptions included

- Pressure gradients are negligible.
- Airflow is fully developed turbulent flow.
- Radiation heat transfer is negligible.
- Air, volatiles, and combustion gases are modeled as a single incompressible ideal gas with a constant molecular weight and a constant specific heat.

Air entrainment was based on a published correlation (Steward, 1970). Volatile combustion with entrained air was assumed to occur instantaneously and homogeneously over the flame cross-section. The heat release rate per unit volume was a function of height only and was determined by conservation of energy. Solving the equations analytically resulted in plots of temperature, plume width, and gas velocity as a function of height above the fuel bed for various levels of firepower, excess air, and volatile fraction.

Building from this earlier work, Bussmann and Prasad published their first coupled cookstove model in 1983 (Bussmann et al., 1983). This model is a steady-state, three-zone model of an open cooking fire composed of (1) a reacting fuel bed zone, (2) a gas phase combustion zone, and (3) a heat transfer zone. The reacting fuel bed zone was modeled as a steady-state, homogeneous top-fed, fixed bed of wood and char with underfire air using a simplified integral model. The fuel bed height and void fraction; fuel size, type, and moisture content; pyrolysis rate of the fuel; and combustion rate of the char were not considered. Instead the heat release rate of the cooking fire was assumed and used to determine the fuel consumption rate, $\dot{m}_f$. Other assumptions within the fuel bed zone included

- The pyrolysis gases are not combusted within the fixed bed of fuel.
- The airflow through the fuel bed (e.g., primary or underfire air) is stoichiometric based on char combustion to CO_2.
- The char yield, y_{char}, is 20% on a dry basis.
- The specific heat of the reactants and products is equal to air.
- The temperature of the top surface of the fuel bed, T_{bed}, is 1100 K.
- The heat of pyrolysis is zero.

The mass flow rate of gases leaving the fuel bed, $\dot{m}_{exit}$, was determined from conservation of mass

$$\dot{m}_{exit} = \left[(1 - y_{char}) + y_{char}\left(\frac{1 + f_{char(s)}}{f_{char(s)}}\right)\right] \tag{7}$$

where $f_{char(s)}$ is the stoichiometric fuel–air mass ratio for char combustion. The exit temperature of the gases, T_{exit}, was determined from the conservation of energy for the reacting bed of fuel

$$y_{char} \dot{m}_f \mathrm{LHV}_{char} = \dot{m}_{exit} c_p (T_{exit} - T_{amb}) + \varepsilon_{bed} \sigma A_{bed} \left(T_{bed}^4 - T_{amb}^4\right). \tag{8}$$

The gas phase combustion zone was modeled using charts developed earlier (Bussmann and Prasad, 1982). Based on the mass flow rate of gases from the reacting bed of fuel, the temperature, plume width, and gas velocity were determined as a function of height above the fuel bed. It was assumed that the presence of the cookpot did not alter the plume of volatiles, and radiant heat transfer to and from the gas phase region was assumed to be negligible. In addition, it was assumed that combustion of volatiles was quenched when reaching the cold cookpot bottom, resulting in unburned volatiles in the exhaust. In the heat transfer zone, radiant heat transfer from the fuel bed to the cookpot bottom was modeled assuming black body radiation between the two surfaces. Convective heat transfer to the cookpot was determined using published correlations (Table 3) for three separate regions of the cookpot, the stagnation region, the bottom beyond the stagnation region, and the sides of the cookpot.

As noted by the authors, the assumption of stoichiometric char combustion led to an overestimation of the temperature of the air leaving the fuel bed. The flame zone model reportedly predicted flame height reasonably well for excess air of 1.5–2.5 without a grate and 2.5–3.5 with a grate. These predictions were based on flame photographs taken during experiments at varying firepower (Prasad et al., 1985). The heat transfer zone model under predicted the heat transfer efficiency. This occurred because

- It was assumed that combustion of the volatiles was quenched at the cookpot bottom.
- The semi-empirical correlations used in the model increased the heat transfer coefficient as the distance between the fuel bed and cookpot increased, which is contrary to experimental observations. This was likely due to using the correlations for a smaller Reynolds number and nozzle-to-plate distances than those for which the relationships were derived (Bussmann, 1988).
- Radiation heat transfer from and to the flame zone was neglected.

Using the same modeling framework as the earlier open fire model, Bussmann and Prasad (1986) modeled a shielded-fire cookstove (Fig. 3). The flow of air and combustion products through the stove was determined by balancing the buoyancy of the hot gases and pressure losses due to flow. The open fire model was updated as follows:

Table 3
Summary of cookpot heat transfer correlations used in modeling of household biomass cookstove modeling.

Model	Pot bottom	Eq.	Ref.	Pot sides	Eq.	Ref.
Enclosed stove						
De Lepeleire et al. (1981)	$20<\tilde{h}<40$ directly above fire $8<\tilde{h}<16$ not directly above fire			$4<\tilde{h}<8$		
Open fire						
Bussmann et al. (1983); Prasad et al. (1985)	Within the stagnation region $\mathrm{Nu}=\frac{\bar{h}D_{plume}}{\tilde{k}}=1.03\ ,\mathrm{Pr}^{0.42}\mathrm{Re}_{D_{plume}}^{0.5}\left(\frac{r}{D_{plume}}\right)^{-0.65}$	(9)	Schlunder and Gnielinski (1967)	$\mathrm{Nu}=0.25\ ,\mathrm{PrRe}^{0.75}\left(\frac{z+12}{W_{jet}}\right)^{-0.6}$	(12)	Seban and Black (1961)
	Beyond the stagnation region			$\frac{T}{T_{jet}}=7.7\frac{\rho_{jet}}{\rho_a}\left(\frac{z+12}{W_{jet}}\right)^{-0.6}$	(13)	Seban and Black (1961)
	$\mathrm{Nu}=0.32\ ,\mathrm{Pr}^{0.33}\mathrm{Re}_{D_{plume}}^{0.7}\left(\frac{r}{D_{plume}}\right)^{-1.23}$	(10)	Hrycak (1978)	$W_{jet}=\frac{\dot{m}_g}{\pi R_{pot}\rho V}$	(14)	Seban and Black (1961)
	$\frac{T-T_{amb}}{T_{pot}-T_{amb}}=0.9\left(\frac{r}{D_{plume}}\right)^{-1.06}$	(11)	Era and Saima (1976)	$\mathrm{Nu}=0.664\sqrt{\mathrm{Re}}$	(15)	Eckert and Drake (1972)
Shielded-fire stove						
Bussmann and Prasad (1986); Baldwin (1987)	Entirely a stagnation point $\mathrm{Nu}_{D_{plume}}=1.26\ ,\mathrm{Pr}^{0.42}\mathrm{Re}_{D_{plume}}\left(\frac{D_{pot}}{D_{plume}}\right)^{-0.5}$	(16)	Shah and London (1978)	Parallel plate with laminar flow $\mathrm{Nu}=1.85\left(\mathrm{Re}\ ,\mathrm{Pr}\frac{2W_{gap}}{H_{sh}}\right)^{1/3}$	(17)	Shah and London (1978)
				Insulated skirt $\mathrm{Nu}=\frac{\tilde{h}\cdot W_{gap}}{\tilde{k}}=4.861$	(18)	Eckert and Drake (1972)
Date (1988)	$\tilde{h}=0.1214\left(\frac{\dot{m}_g}{A_{gap}D_c}\right)^{1/2}$	(19)	Bhandari et al. (1988)	Loss from top $\tilde{h}_{top,loss}=1.3\left(\frac{T_{pot}-T_{amb}}{D_{pot}}\right)^{0.25}$	(20)	
				Loss from sides as vertical heated plate $\tilde{h}_{side,loss}=1.42\left(\frac{T_{pot}-T_{amb}}{H_{pot}}\right)^{0.25}$	(21)	
Shah and Date (2011)	$\mathrm{Nu}=0.5(1.65\mathrm{Re}_D^{0.5}+2.733\mathrm{Re}_D^{0.59})$	(22)	Bhandari et al. (1988)	Eq. (21)		

$\tilde{h}$ is in units of $\mathrm{W/m^2\cdot K}$

- Black body radiation heat transfer was assumed to be between an infinitely thin fuel bed, the stove surfaces, and the cookpot surfaces.
- The temperature of the stove surfaces was determined from experiment (Visser, 1984).
- The temperatures of the fuel bed and the exiting gases were assumed to be equal.
- Radiation losses from the flames to the stove body were assumed to be 17% of the heating value of the volatiles.
- In the heat transfer zone, the flow field was similar to that of the open fire model and included air entrainment due to the large secondary air holes. The cookpot shield was assumed to be of constant temperature and equal to the cookpot temperature. Radiation heat transfer into the cookpot was modeled as a constant 13% of the heat liberated by combustion.

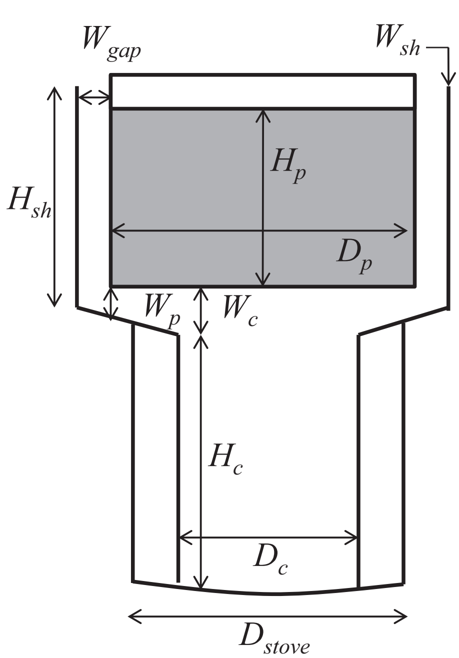

Fig. 3. Cookstove dimensions.

As in the open fire model, the fuel consumption rate was determined using the heat release rate. Conservation of mass and conservation of energy were used to determine the mass flow rate of air and the temperature of the exiting gases, respectively. In the heat transfer zone, the convective heat transfer to the cookpot bottom was modules assuming that the entire cookpot bottom was within the stagnation region (Eq. (16)). Convective heat transfer to the cookpot sides modeled based on a heat transfer coefficient for flow between two parallel annular plates of equal temperature (cookpot and shield) with hydrodynamically fully developed flow but thermally developing flow (Eq. (17)) (Shah and London, 1978). The resulting set of 14 algebraic equations was solved to calculate excess air, temperature, and heat transfer for varying geometrical and firepower parameters. Solutions resulting in excess air less than one or greater than ten were rejected. It was found that for a given fire power there was an optimum gap between the cookpot and the stove shield. Gaps smaller than the optimum resulted in fuel rich combustion, whereas gaps larger than the optimum rapidly increased the excess air, decreasing combustion temperatures and thermal efficiency. The model prediction agreed with the experiments near the optimum gap width, but it over-predicted the sensitivity of the efficiency to decreasing and increasing gap width as well as the minimum permissible gap.

To briefly summarize the Eindhoven modeling effort, two separate but related models were developed—an open fire model applicable to three-stone stoves and a shielded-fire cookstove model. In both cases the heat release rate of the cookstove was assumed, and the processes occurring within the three major zones of the cookstove system—the reacting fuel bed zone, the gas phase combustion zone, and the heat transfer zone around the cookpot—were coupled together. This coupling occurred through heat transfer between the zones and the airflow rate. Specifically, the fuel bed temperature was using an energy balance that included the combustion rate, airflow rate, and radiation heat transfer from the top surface of the bed. Heat transfer to the cookpot was based on convection from the flame zone, and radiation from the stove body and reacting fuel bed. The airflow was based on the buoyant flow of gases and flow losses in the stove. In addition to the modeling efforts above, the transient heat flow through stove walls of varying materials was modeled (Prasad et al., 1985). This study found that an insulated stove wall with low thermal capacity increased efficiency by reducing the heat lost due to storage in the thermal mass of the stove.

Kumar, Lokras, and Jagadish also developed a coupled model with no explicit gas phase combustion in 1990 (Kumar et al., 1990). Steady-state heat transfer in a three-cookpot enclosed-fire cookstove was modeled through energy balances using a series of six well-stirred reactors to examine the effects of geometry on efficiency and to compare the fraction of thermal energy reaching the pots versus body and exhaust losses. The modeling assumptions included

- The cookstove operates at a steady state with a constant wood consumption rate, charcoal production rate, and excess air.
- Combustion of volatiles is complete.
- Pyrolysis is complete.
- The chamber under each of the pots is a hemispherical volume; the three chambers and the chimney are connected serially with rectangular ducts. The six volumes (three chambers and three ducts) are well-stirred reactors with instant mixing, uniform velocity, and uniform gas temperature equal to the exit and the wall temperatures.

The gas temperature leaving the fuel bed as an input to the series of reactors was determined using an energy balance in which the lower heating value of the dry wood minus the lower heating value of the unburned charcoal was equal to the heat of vaporization of the fuel moisture and sensible heat of the hot combustion products for the given excess air. Convective heat transfer to the cookpot bottoms was modeled using published heat transfer correlations for laminar flow through a rectangular duct of a given geometry (Clark and Kays, 1953)

$$\frac{\mathrm{Nu}}{\mathrm{Nu}_\infty} = 1 + \left(0.003 + 0.039\frac{W}{H}\right)\frac{D_H}{L}\mathrm{Re}\,\mathrm{Pr} \tag{23}$$

where Nu_∞ is the asymptotic value available as a curve fit as a function of the width, W, and height, H, of the duct for air, Nu is the average Nusselt number for the pot bottom, and $D_H$is the hydraulic diameter.

Radiative transfer from the wall to the cookpot was evaluated assuming view factors based on a simplified geometry of gray concentric spheres. The radiative heat transfer coefficients from the participating gas media to each cookpot were determined from charts in the literature (Trinks et al., 2003) as a function of the partial pressure of CO_2 and H_2O, the gas temperature, and the beam length, which was increased by a factor of 1.1 when the gas is luminous. Conductive losses to the spherical mud walls were modeled as cumulative loss per small time elements to represent the steady-state condition through solution of the transient conduction equation (Carslaw and Jaeger, 1959). The sensible energy leaving each well-stirred reactor was the sum of the specific heats of the gases.

To determine the excess air, the buoyant flow of the chimney draft was set equal to the pressure drop through the flow path. The chimney temperature distribution was determined from the overall energy balance in the chimney by using the thermal resistance method with the interior heat transfer coefficient calculated using an empirical correlation for turbulent flow

$$\mathrm{Nu} = 0.023\mathrm{Re}^{0.8}\,\mathrm{Pr}^{0.3}. \tag{24}$$

Pressure losses through the geometries were evaluated using published pressure loss coefficients. The model showed overall agreement with experiment; however, the model predicted higher heat transfer into the first cookpot relative to the subsequent cookpots. The model predicted that convective transport and radiative transport play equal roles in heat transfer into the cookpots.

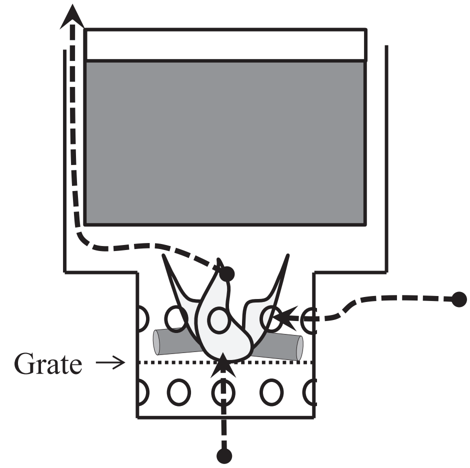

Fig. 4. Shielded-fire cookstove modeled by Bussmann and Prasad (Bussmann and Prasad, 1986).

Coupled models with explicit gas phase combustion

Using similar assumptions to the Eindhoven models, Date developed a detailed three-zone model of heat transfer in a shielded-fire stove with a nozzle contraction above the fuel bed and primary and secondary air (Fig. 4) (Date, 1988). The reacting fuel bed was modeled using time-averaged rates of pyrolysis and char burning that accounted for fuel diameter and moisture content based on experimental measurements of temperature and weight-loss histories (Tinney, 1965; Blackshear and Murthy, 1965). Gas flow was modeled via buoyancy and pressure losses. The effect of swirl on the heat transfer rate was investigated by multiplying by a factor of 1.0–1.5 to increase the coefficient of heat transfer to the cookpot and the pressure loss coefficients. In contrast to earlier models (other than Baldwin (1987)), this model incorporated additional geometrical complexity, losses through the walls, and participating media (Date, 1988). (See Fig. 5.)

In the fuel bed zone, a simplified packed model was introduced. The steady-state solid phase combustion was modeled for burning large (0.5–5 cm diameter) wood by determining the time-averaged outputs of pyrolysis and char burning based on the wood surface temperature, T_{wood}, and energy balance at the wood surface assuming

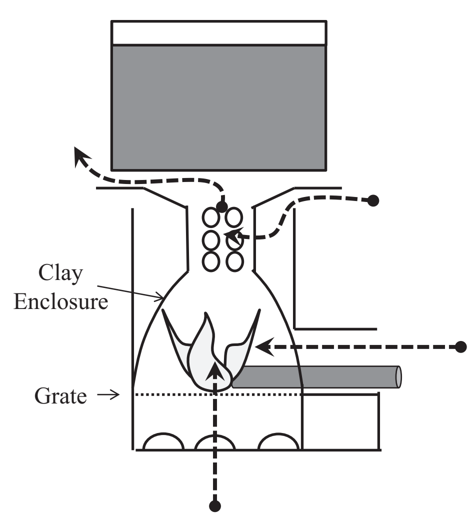

Fig. 5. Shielded-fire stove modeled by Date and Shah (Date, 1988; Shah and Date, 2011).

Table 4
Summary of rate constants for wood pyrolysis used in modeling of household biomass cookstove modeling.

Model	$k_{0,pyr}$ (s^{-1})	E_{pyr} (kcal/g mol)
Prasad et al. (1985)	7×10^7	30.1
Date (1988)		
−2.54 cm dia wood	6×10^7	29.8
−1.26 cm dia wood	3.5×10^8	29.8
−0.63 cm dia wood	7.5×10^8	29.8
Shah and Date (2011), curve fit from Date (1988)[a]	$(3541.2D_{wood}–13.625) \times 10^7$	29.8

[a] D_{wood} is the diameter of the wood in meters

- The wood was fed into the stove at an exact burning rate with a constant given burning surface area, A_{wood} (typically 400 cm^2) and steady-state operation.
- For the initial 40% of the time, the production of pyrolysis gases dominated at a lower surface temperature ($T_s = T_{wood} - 50$). For the remaining 60% of the time, char burn dominated with a higher surface temperature ($T_s = T_{wood} + 50$) (Tinney, 1965; Blackshear and Murthy, 1965).
- Radiation between the wood surface and the stove enclosure was determined considering the participating medium as a function of mean beam length and temperature.
- The heat of pyrolysis was taken from the literature as

  $$h_{pyr} = 10.47(4926D_{wood} + 38)\text{kJ/kg}$$

  where D_{wood} is the diameter of the wood in meters (Simmons and Lee, 1985).
- The mass fraction of the volatiles was varied from 0.6 to 0.9.

The mass burning flux of wood was assumed to be kinetically controlled and was determined based on the time-averaged steady-state pyrolysis of the wood and combustion of the char. Both the wood pyrolysis rate and the char combustion rate were expressed as Arrhenius relationships in which the constants were evaluated in terms of the wood diameter, as shown in Tables 4 and 5, respectively.

$$\dot{m}''_f \simeq \frac{\rho_{wood} D_{wood}}{4}\left(\frac{0.4y_{vol}k_{0,pyr}e^{-E_{pyr}/\hat{R}T_{pyr}} + 0.6y_{char}k_{0,char}e^{-E_{char}/\hat{R}T_{char}}}{2}\right) \tag{25}$$

The wood surface temperature was determined through an integral energy balance that included convective and radiative heat transfer and the change in energy storage within the material based on an inner temperature of 150° below the wood surface temperature (Evans and Emmons, 1977).

$$\dot{m}''_f\left(c_{p,g}(T_s - T_{amb}) - c_{p,wood}(T_s - 150 - T_{amb}) - h_{pyr}\right) = q_{rad} + q_{conv} \tag{26}$$

Table 5
Summary of char combustion rate constants used in household biomass cookstove modeling.

Model	$k_{0,char}$ (s^{-1})	E_{char} (kcal/g mol)
Date (1988)		
−2.54 cm dia wood[a]	4×10^8	42.7
−1.26 cm dia wood[a]	1.2×10^9	39.5
−0.63 cm dia wood[a]	2×10^9	36.3
Shah and Date (2011), curve fit from Date (1988)[b]	$(8071.94D_{wood}–0.619) \times 107$	$332.9D_{wood} + 34.26$

[a] Charcoal produced from wood of given diameter.
[b] D_{wood} is the diameter of the wood which produced the char in meters.

A heated cylinder correlation was used to determine q_{conv} (Holman, 2009); q_{rad} and other radiative transfers were determined from the geometry and included participating media where transmissivities and emissivities were evaluated as functions of mean beam length and temperature evaluated at 700 K.

$$\tau_{i\to j} = 1 - \varepsilon_{i\to j} \tag{27}$$

$$\varepsilon_{i\to j} = \exp\left[\left(0.848 + 9.02 \times 10^{-4}T\right) + \left(0.9589 + 4.8 \times 10^{-6}T\right)\ln(0.2L_{beam})\right] \tag{28}$$

$$L_{beam} = 3.6\frac{V}{A_s} \tag{29}$$

Primary and secondary airflow rates were determined using the correlations given in Table 6 for pressure losses through stove geometries including inlet holes, expansions, and bends. Heat losses through the stove walls were determined using a thermal resistance analog similar to Baldwin (1987) including conduction, convection, and radiation where the convective heat transfer coefficients were taken as 5 or 6 W/m^2 K depending on location. In the heat transfer zone, the heat transfer correlations around the cookpot are listed in Table 3. Heat transfer from the cookpot bottom was taken from experiment (Bhandari et al., 1988). Heat transfer from the sides of the cookpot was modeled as the convective loss of a vertical heated plate at a cookpot temperature ($T_{pot} = 343 \pm 5$ K).

This model (Date, 1988) was updated by Shah and Date (2011) to incorporate gas phase combustion. In the original model, complete combustion and heat release, calculated as the product of the fuel burning rate and heating value of fuel, was assumed to occur in the fuel bed. The later model uses a simplified four-step global reaction mechanism (Hautman et al., 1981) to model the combustion of volatiles by dividing the reacting gas phase zone into a series of five geometrically-distinct well-stirred reactors (Shah and Date, 2011). These are (1) the primary air inlets under and through the grate, (2) the bed zone, (3) the nozzle-shaped area above the bed zone, (4) the cylinder with secondary air holes, and (5) the expansion under the cookpot. The mass flow and mass fraction of the products of pyrolysis and char combustion exiting the bed zone were determined using a generic formula for wood composition (Tillman et al., 1981) and assuming that the pyrolysis products of dry wood consisted of CO_2, CO, H_2, H_2O, and C_7H_{16} (C_7H_{16} was used to represent both the light and heavy hydrocarbons). Based on a mass balance of the elements, it was assumed that the mass ratio of CO to CO_2 and H_2O to CO_2 in the volatiles exiting the fixed bed was 1.591 and 2.174, respectively (Ragland et al., 1991). From this the mass rate of flow of each pyrolysis gas species, j, is expressed as a function of moles and molecular weight of that species

$$\dot{m}_{j,vol} = \dot{m}_{vol}\left(n_j\frac{M_j}{M_{vol}}\right). \tag{30}$$

Table 6
Minor pressure loss coefficients for stove geometries (Date, 1988; Shah and Date, 2011).

Contraction[a]	$K_{cont} = 0.5\ ,\sin\phi\left(1 - \frac{A_{i+1}}{A_i}\right)$	(35)
Expansion	$K_{exp} = \left(1 - \frac{A_i}{A_{i+1}}\right)^2$	(36)
Bend	$K_{bend} = 1.0$	
Entry through primary air holes	$K_{in} = 0.6$	
Grate with spacing W_{grate} and rod diameter D_{rod} (Kazantsev, 1977)	$K_{grate} = 0.75\left(\frac{W_{grate}+D_{rod}}{D_{rod}} - 1\right)^{1.33}$	(37)
Fuel bed	$K_{bed} = 1.12(0.66N_{row} + 0.5)$ $K_{bed} = 1.3$	(38)
Under pot bottom with gap A_{gap} (Bussmann and Prasad, 1986)	$K_{pot,bottom} = \left[\left(\frac{A_{pot}}{A_{gap}}\right)^2 - 1\right] + \left[\left(\frac{A_{pot}}{A_{gap}}\right) - 1\right]^2$	(39)

[a] is the half-angle of the contraction.

The char combustion products were determined by assuming a one-step surface reaction of C and O_2 to CO_2. Combining the pyrolysis gases, char combustion products and the fuel moisture yields

$$\dot{m}_{\mathrm{CO_2}} = \dot{m}_{\mathrm{char}}\left(\frac{M_{\mathrm{CO_2}}}{M_{\mathrm{char}}}\right) \tag{31}$$

$$\dot{m}_{\mathrm{O_2}} = -\dot{m}_{\mathrm{char}}\left(\frac{M_{\mathrm{O_2}}}{M_{\mathrm{char}}}\right). \tag{32}$$

Incorporating the gas phase reactions and the secondary airflow into the species and energy balances for each of the well-stirred reactors, *i*, yields

$$y_{j,i} = \frac{\dot{m}_{i-1}y_{j,i-1} + \dot{m}_{air}y_{j,amb} + r_{j,i}\left(T_i, y_{j,i}\right)\forall_i}{\dot{m}_{g,i}} \tag{33}$$

$$q_{vol,i} = \sum r_{j,i}\left(T_i, y_{j,i}\right)\mathrm{LHV}_j\forall_i. \tag{34}$$

From this coupled equation set, the temperature and mass fraction of species can be determined. Combustion efficiency was then evaluated as the sum of char and volatile heat release in each zone divided by the total fuel energy feed rate. The mass flow rate of each species at the exit of the stove divided by the mass flow rate of fuel is also reported.

The model was used to investigate the effect of nine geometrical design variables and three operational parameters on steady-state thermal and combustion efficiencies. Results from the Date model (Date, 1988) predicted an efficiency of 0.36% less than the efficiency that was measured in a concurrent experiment (Bhandari et al., 1988) and the published fuel burning rate (Blackshear and Murthy, 1965). The Shah and Date model (Shah and Date, 2011) predicted efficiency to be 1.2% higher than the same experiment, and excess air and stove power were in close agreement. The CO/CO_2 ratio was predicted at 0.17 compared to 0.12–0.16 as measured in Bussmann and Prasad (Bussmann and Prasad, 1986), and the airflow rate and surface temperature of the wood were in good agreement with Kausley and Pandit (2010).

Coupled CFD models

In 2003 Weerasinghe and Kumara (2003) used a three-dimensional, steady-state, reacting flow CFD model to examine temperature, velocity, and emissions profiles in a cylindrical combustion chamber below a flat cooking plate. The source term of energy release due to gas phase combustion was approximated by the reaction rate of fuel combustion taken as the slowest of the dissipation rates of fuel, oxygen, and products. The gas phase heat release rate was assumed to be 3 kW, which was 75% of the total stove power (gas phase and char phase combustion). The predicted temperature was 100–300 K lower than experimentally measured temperature.

Gupta and Mittal (2010a) developed a two-dimensional, axisymmetric, steady-state CFD model to examine heat transfer in the wood-burning Janta stove. Flow through the fuel bed was modeled as a porous medium using the Darcy–Brinkman equation with effective bed thermal conductivity as a weighted average based on porosity. Forty percent of the heat release was assumed to occur in the bed zone, and the remaining 60% of the heat release was assumed to occur in the flame zone. Combustion was treated as a uniformly distributed source term with no prediction of species concentrations. The permeability of the fuel bed was expressed through the Karman–Cozeny relationship. Pyrolysis rates were determined experimentally and represented as pseudo first order reactions based on temperature in Gupta and Mittal (2010b) and modeled as a uniform heat release rate. The model was validated with 5% and 10% agreement with two cases from the literature (Kageyama and Izumi, 1970; Kohli, 1992).

In 2008 Burnham-Slipper incorporated an analytical model for heat transfer based on jet impingement on a flat plate (Burnham-Slipper et al., 2007a) and an analytical model for simplified packed bed wood combustion (Burnham-Slipper et al., 2007b) into a two-dimensional, axisymmetric, steady-state CFD model (Burnham-Slipper, 2008). This model was used to optimize an African rocket-type griddle stove. The simplified packed bed model for thermally thick wood combustion assumed that pyrolysis is limited by the rate of heat transfer through the fuel and that char combustion is limited by the rate of oxygen diffusion. The pyrolysis and char combustion rates were then based on matching the experimental burn rate and temperature field in a crib of stacked cylindrical fuel with varying volume, void fraction, and specific area, thus introducing a lumpiness function to incorporate mixing of discrete streams of volatiles and oxidants.

Char combustion to CO_2 was modeled using oxygen diffusion through the species boundary layer according to Fick's law and assuming O_2 is fully consumed and experimentally shown to be limited by diffusion resulting in the simplified oxygen consumption rate

$$\dot{m}'''_{\mathrm{O_2}} = -\frac{a}{v}h_m\rho_{\mathrm{O_2},\infty}. \tag{40}$$

Here *a* is the fuel specific area (m^2/m^3), *v* is the normalized crib volume, and units of volume specific mass flow are kg/m^3 s. The mass transfer coefficient for flow through an inert packed bed of particles of diameter D is given by Cussler (2009)

$$\frac{h_m}{V_0} = 1.17\left(\frac{DV_0}{v}\right)^{-0.42}\left(\frac{D_{AB}}{v}\right)^{0.66} \tag{41}$$

which was simplified as approximately proportional to the square root of the superficial velocity, $\sqrt{V_0}$. The simplified char combustion model then became

$$\dot{m}'''_{char} = \frac{12}{32}\frac{a}{v}h_mV_0^{0.5}\rho_{\mathrm{O_2},\infty} \tag{42}$$

$$\dot{m}'''_{\mathrm{CO_2}} = \frac{44}{32}\frac{a}{v}h_mV_0^{0.5}\rho_{\mathrm{O_2},\infty} \tag{43}$$

$$q'''_{char} = HHV_{char}m'''_{char}. \tag{44}$$

Pyrolysis was modeled with drying and volatile release as a superimposed single thermal decomposition wave based on Bryden et al. (2002) assuming a constant pyrolysis temperature of 550 K (Demirbas, 2004) and a pyrolysis wave separating char and virgin wood surfaces at varying radius *r* for fuel of radius *R*. The heat conducted through the char layer is

$$q'''_{pyr} = \frac{\tilde{k}_{char}a\left(T - T_{pyr}\right)}{vR\ln\left(\frac{R}{r}\right)}. \tag{45}$$

The resulting mass flow of volatiles was determined by dividing q'' by the effective heat of pyrolysis, including sensible energy from the temperature rise, which was estimated as 2.5 MJ/kg_{vol} based on experimental values. The mass flow of water and volatiles were then calculated per their mass fraction from proximate analysis. Values of inertial flow resistance coefficient for the crib were calculated from the Ergun equation and verified experimentally.

In the flame region, chemistry was modeled using the species-transport model of Fluent™ (ANSYS Inc., 2005) where the reaction between wood volatiles and oxygen was

$$CH_2O + O_2 \rightarrow CO_2 + H_2O$$

and was limited by turbulent mixing according to the eddy-dissipation model.

Radiation heat transfer was included using the discrete ordinates method and weighted-sum-of-gray-gases model. No model was available for soot production; as a result the effect of particulate soot was not included. Convective heat transfer to the griddle plate was modeled as a steady-state axisymmetric impinging jet with turbulence while neglecting the effects of buoyancy and radiation and was validated experimentally. The zones were then coupled. The model was validated experimentally, and it identified the trends of fuel burn rate and heat transfer correctly. However, agreement with experimental data was poor. The model was shown by the authors to be insensitive to changes in stove height and overly sensitive to changes in diameter.

Single aspect models

In addition to the models discussed above, several models have focused on only one aspect of household biomass cookstove performance. Schutte et al. (1991) discuss prediction of flue gas composition for constant firepower in an enclosed-fire stove. Several studies used CFD and assumed non-reacting hot gases to model only the heat transfer zone at the cooking surface; these include Bryden et al. (2003) who optimized baffle designs in enclosed-fire cookstoves and Wohlgemuth et al. (2010) and Joshi et al. (2012) who studied heat transfer within a cookpot shield. Agenbroad et al. (2011a,b) created a simplified model of natural convection in a shielded-fire, idealized "rocket" elbow, assuming

- Constant given firepower with a perfectly efficient and instantaneous heat addition and no distinction between the fuel bed (char) and flame (volatile) combustion
- One-dimensional flow in an isobaric system with no work and constant potential energy
- Incoming air and combustion products modeled as an unspecified ideal gas with constant specific heat
- Adiabatic stove walls, noting that in reality approximately 1/3 of the heat is lost through the walls
- No cookpot present.

The heat released by a given firepower was used to determine the flame temperature in terms of the average specific heat of the mass flow of air (Eq. (46)). As in previous models, Bernoulli's equation for compressible flow was used to determine the mass flow rate of air (Eq. (47)) with a variable loss coefficient, $0 \le C \le 1$, introduced to account for uncertainties and inefficiencies in the buoyant flow.

$$q = \dot{m}_{air}\bar{c}_p\left(T_{flame} - T_{amb}\right) \tag{46}$$

$$\dot{\forall}_{air} = CA_c\sqrt{2gH_c\left(\frac{T_{flame} - T_{amb}}{T_{amb}}\right)} \tag{47}$$

Eqs. (46) and (47) were solved simultaneously to determine $T_{flame}$and excess air with the product $CA_c\sqrt{H_c}$ taken as the variable geometric parameter. Based on this, dimensionless forms of temperature, mass flows of air and fuel, and heating value were proposed for use in design tools.

Conclusions

The goal of cookstove modeling is to develop a complete, validated computational model that can be used to improve the design of household biomass cookstoves used by the more than 2.4 billion people in the developing world. To meet this need a model (or set of models) is needed that

- is validated across a range of common geometries and operating conditions,
- can size the flow of primary and secondary air,
- couples heat transfer with gas phase and solid phase combustion,
- can account for heat losses to the environment, stove body, and cookpot or surface,
- can model variations in fuel type, size, and feed rate,
- accounts for packed bed combustion with and without a grate,
- predicts particulate and gaseous emissions, and
- includes the effects of operator actions (e.g., method of tending and cooking strategies).

As shown in this review, significant progress has been made in developing the pieces of such a model, and these modeling efforts can be used to quantitatively and qualitatively guide stove design in improving stove heat transfer and overall efficiency. However, more work is needed to better understand and characterize the heat transfer and combustion processes within traditional household biomass cookstoves. This includes modeling of transient processes such as the addition of fuel charges, start-up, and cool-down. In the packed bed zone, models of drying, pyrolysis, and char combustion for various fuel sizes, shapes, and arrangements need to be addressed; and models of particulate release need to be developed. In the gas phase zone, detailed models of heat release and heat transfer and of particulate and gaseous emissions, particularly those of polycyclic aromatic hydrocarbons and soot, are needed. In the heat transfer zone, models that include radiation with a participating medium including gas composition and particle concentration within the gas and luminous flames are needed, as well as validated convective heat transfer correlations specific to the flow and temperature regimes for the various regions within the stove body and cooking surfaces. Beyond this, a framework needs to be developed to support the creation of an integrated and detailed model of traditional household biomass cookstoves that can be used in engineering design.

In addition, a broad data set of validation data is needed to support model development; therefore, the data required for model development should be considered and included when publishing results of experiments. Finally, it should be recognized that performance in the field under highly varied conditions may be different than performance in the laboratory or predicted by any model. Efforts are needed to develop the narrative and quantitative data needed to understand how improved household biomass cookstoves fit as a village energy intervention and to link the design of the stove with the desired personal and village scale outcomes.

Similar models need to be developed for other types of cookstoves, including those with forced draft or those utilizing prepared fuels such as pellets and charcoal. Modeling these household cookstoves has received less attention than modeling the natural draft wood burning cookstoves discussed here, along with those burning other types of biomass fuels such as dung cakes and crop residues. However, a few models have been developed for prepared fuel stoves (Varunkumar et al., 2012; Ravi et al., 2002, 2004; Chaney et al., 2009; Dixit et al., 2006a,b), and charcoal stoves (Khummongkol et al., 1988). These models need to be more fully developed and extended to provide a broad range of cookstove design options for the developing world.

Nomenclature

a	fuel specific area, m^2/m^3
A	area, m^2
c_p	specific heat kJ/kg·K
C	constant
D	diameter, m
D_{AB}	binary diffusion coefficient, m^2/s
D_H	hydraulic diameter, m
E	activation energy in the Arrhenius form of a reaction rate, kJ/kg mol

F	view factor
f	fuel–air mass ratio
g	gravity, m/s^2
H	height, m
h	specific enthalpy, kJ/kg
$\tilde{h}$	convective heat transfer coefficient, W/m^2·K
h_{pyr}	heat of pyrolysis, kJ/kg
h_m	mass transfer coefficient, m/s
i	counter
j	counter
k	kinetic rate constant, units vary
$\tilde{k}$	thermal conductivity, W/m·K
K	minor pressure loss coefficient
L	length, m
$\dot{m}$	mass flow rate, kg/s
$\dot{m}''$	mass flow rate per unit area kg/m^2·s
$\dot{m}'''$	mass flow rate per unit volume kg/m^3·s
N_{row}	number of rows of wood pieces in the fuel bed
q	heat transfer rate, W
q'''	heat transfer rate per unit volume, W/m^3
r	rate of species production or destruction, kg/m^3·s; radius, incremental, m
R	radius, fixed, m
$\hat{R}$	universal gas constant, kJ/kg mol·K
T	temperature, K
t	time, s
V	velocity, m/s
$\forall$	volume, m^3
$\dot{\forall}$	volumetric flow rate, m^3/s
v	normalized crib volume
W	width, m
y	mass fraction
Δz	segment height, m
β	fuel bed size factor
δ	gap width, m
ε	emissivity
ϕ	half-angle of contraction
υ	kinematic viscosity, m^2/s
ρ	density kg/m^3
σ	Stefan–Boltzmann constant, W/m^2·K^4
τ	transmissivity

Dimensionless numbers

Nu	Nusselt number
Pr	Prandtl number
Re	Reynolds number

Abbreviations

HHV	higher heating value, kJ/kg
LHV	lower heating value, kJ/kg

Subscripts

air	air
amb	ambient
bed	fuel bed
bend	bend
c	combustion chamber
char	char
cont	contraction
conv	convection
exp	expansion
ext	exterior wall
f	fuel
flame	flame
g	gas
gap	gap
grate	grate
in	inlet
int	interior wall
jet	the plume of hot gases rising up the side of the pot
plume	the plume of hot gases rising from the burning fuel, the flame
pot	pot
pyr	pyrolysis
rad	radiation
(s)	stoichiometric
s	surface
sh	shield
side	pot side
stove	stove
top	pot top
tot	total
vol	volatiles
wall	wall
wood	wood
∞	freestream

Acknowledgments

The authors gratefully acknowledge the financial support of Nordica MacCarty by the United States National Science Foundation Graduate Research Fellowship Program (Grant no. DGE0751279).

References

Agenbroad J, DeFoort M, Kirkpatrick A, Kreutzer C. A simplified model for understanding natural convection driven biomass cooking stoves—part 1: setup and baseline validation. Energy Sustain Dev 2011a;15(2):160–8.
Agenbroad J, DeFoort M, Kirkpatrick A, Kreutzer C. A simplified model for understanding natural convection driven biomass cooking stoves—part 2: with cook piece operation and the dimensionless form. Energy Sustain Dev 2011b;15(2):169–75.
ANSYS Inc. Fluent version 6.2; 2005.
Baldwin SF. Biomass stoves: engineering design, development and dissemination. [dissertation]. Princeton (NJ): Princeton University Center for Energy and Environmental Studies, Princeton; 1987.
Bhandari S, Gopi S, Date A. Investigation of CTARA wood-burning stove; part I—experimental investigation. Proc Indian Acad Sci 1988;13:271–93.
Blackshear PL, Murthy KA. Heat and mass transfer to, from and within cellulosic solids burning in air. 10th Symp (Intl) Comb; 1965. p. 911–23.
Bond TC, Doherty SJ, Fahey DW, Forster PM, Berntsen T, DeAngelo BJ, et al. Bounding the role of black carbon in the climate system: a scientific assessment. J Geophys Res-Atmos 2013;118(11):5380–552.
Bruce N, Rehfuess E, Mehta S, Hutton G, Smith K. Indoor air pollution. In: Jamison DT, Breman JG, Measham AR, Alleyne G, Claeson M, Evans DB, editors. Disease control priorities in developing countries. 2nd ed. New York: Oxford University Press; 2006. p. 793–816.
Bryden KM, Ragland KW, Rutland CJ. Modeling thermally thick pyrolysis of wood. Biomass Bioenergy 2002;22:41–53.
Bryden KM, Ashlock DA, McCorkle DS, Urban GL. Optimization of heat transfer utilizing graph based evolutionary algorithms. Int J Heat Fluid Flow 2003;24:267–77.
Burnham-Slipper H. Breeding a better stove: the use of computational fluid dynamics and genetic algorithms to optimise a wood burning stove for Eritrea [dissertation]. Nottingham, UK: University of Nottingham; 2008.
Burnham-Slipper H, Clifford MJ, Pickering SJ. Jet impingement heat transfer for low nozzle-to-plate clearances. Proc 10th UK Natl Heat Transfer Conf; 2007a.
Burnham-Slipper H, Clifford MJ, Pickering SJ. A simplified wood combustion model for use in the simulation of cooking fires. Proc HEFAT; 2007b.
Bussmann P. Woodstoves: theory and applications in developing countries [dissertation]. Eindhoven: Eindhoven University of Technology; 1988.
Bussmann PJT, Prasad K. Model predictions of temperature and velocity profiles in turbulent diffusion buoyant flames. Proc 7th Int Heat Transfer Conf; 1982.
Bussmann P, Prasad KK. Parameter analysis of a simple woodburning cookstove. Proc 8th Intl Heat Transfer Conf, 6. ; 1986. p. 3085–90.
Bussmann PJT, Visser P, Prasad K. Open fires: experiments and theory. Proc Indian Acad Sci Sect C 1983;6(1):1–34.
Carslaw HS, Jaeger JC. Heat conduction in solids. 2nd ed. London: Oxford University Press; 1959. p. 246.
Chaney J, Wilson R, Clifford MJ. Development of a semi-empirical model for the combustion of low-density biomass briquettes for use in the simulation of cookstoves. Proc ECM 2009;2009.
Clark SH, Kays WM. Laminar-flow forced convection in rectangular tubes. Trans ASME 1953;75:859–66.
Cussler EL. Diffusion: mass transfer in fluid systems 3rd ed. Cambridge: Cambridge University Press; 2009.

Date A. Investigation of CTARA wood-burning stove. Part II. Analytical investigation. Proc Indian Acad Sci 1988;13(4):295–317.
De Lepeleire G, Christiaens M. Heat transfer and cooking woodstove modelling. Proc Indian Acad Sci 1983;6(1):35–46.
De Lepeleire G, Prasad KK, Verhaart P, Visser P. A woodstove compendium. Eindhoven, The Netherlands: Eindhoven University of Technology; 1981.
Demirbas A. Combustion characteristics of different biomass fuels. Prog Energy Combust Sci 2004;30:219–30.
Dixit CSB, Paul PJ, Mukunda HS. Part I: experimental studies on a pulverized fuel stove. Biomass Bioenergy 2006a;30:673–83.
Dixit CSB, Paul PJ, Mukunda HS. Part II: computational studies on a pulverized fuel stove. Biomass Bioenergy 2006b;30:684–91.
Eckert ERG, Drake RM. Analysis of heat and mass transfer. New York: McGraw-Hill; 1972.
Era Y, Saima A. An investigation of impinging jet—experiments by air, hot air and carbon dioxide. Bull JSME 1976;19:800–7.
Evans DD, Emmons HW. Combustion of wood charcoal. Fire Res 1977;1:57–66.
Gupta R, Mittal ND. Fluid flow and heat transfer in a single-pan wood stove. Int J Eng Sci Techol 2010a;9:4312–24.
Gupta R, Mittal ND. Pyrolysis modelling in a wood stove. Int J Eng Sci Technol 2010b; 2(10):5088–98.
Hautman DJ, Dryer FL, Schug KP, Glassman I. A multiple-step overall kinetic mechanism for the oxidation of hydrocarbons. Combust Sci Technol 1981;25:219–35.
Holman JP. Heat transfer. 10th ed. New York: McGraw-Hill; 2009.
Hrycak P. Heat transfer from a row of jets impinging on concave semi-cylindrical surface. Proc 6th Int Heat Transfer Conf; 1978. p. 67–72.
Incropera FP, DeWitt DP, Bergman TL, Lavine AS. Fundamentals of heat and mass transfer. 6th ed. John Wiley & Sons; 2007.
International Energy Agency (IEA). Energy poverty: how to make modern energy access universal? Paris: World Energy Outlook; 2010.
Jetter J, Zhao Y, Smith KR, Khan B, Yelverton T, DeCarlo P, et al. Pollutant emissions and energy efficiency under controlled conditions for household biomass cookstoves and implications for metrics useful in setting international test standards. Environ Sci Technol 2012;46:10827–34.
Johnson NG, Bryden KM. Energy supply and use in a rural west African village. Energy 2012;43:283–92.
Joshi J, Pandit AB, Patel SB, Singhal RS, Bhide GK, Mariwala KV, et al. Development of efficient designs of cooking systems. II. Computational fluid dynamics and optimization. Ind Eng Chem Res 2012;51:1897–922.
Kageyama M, Izumi R. Natural heat convection in a vertical circular tube. Bull JSME 1970; 13:382–94.
Kausley SB, Pandit AB. Modelling of solid fuel stoves. Fuel 2010;89:782–91.
Kazantsev EI. Industrial furnaces. Moscow: Mir Publishers; 1977.
Khummongkol P, Wibulswas P, Bhattacharya SC. Modeling of a charcoal cook stove. Energy 1988;13(11):813–21.
Kohli S. Buoyancy induced flow and heat transfer in biomass stoves [dissertation]. Bangalore: Bangalore Indian Institute of Science; 1992.
Kumar R, Lokras SS, Jagadish KS. Development, analysis & dissemination of a 3-pan cookstove. Indian Institute of Science: Bangalore; 1990.
Legros G, Havet I, Bruce N, Bonjour S. The energy access situation in developing countries. World Health Organization and UNDP; 2009.
Lim SS, Vos T, Flaxman AD, Danaei G, Shibuya K, Adair-Rohani H, et al. A comparative risk assessment of burden of disease and injury attributable to 67 risk factors and risk factor clusters in 21 regions, 1990–2010: a systematic analysis for the Global Burden of Disease Study 2010. Lancet 2012;380:2224–60.
MacCarty N, Still D, Ogle D. Fuel use and emissions performance of fifty cooking stoves in the laboratory and related benchmarks of performance. Energy Sustain Dev 2010;14: 161–71.
Prasad KK, Sangen E, Visser P. Woodburning cookstoves. In: Hartnett JP, Irvine TF, editors. Advances in Heat Transfer, 17. Elsevier; 1985. p. 159–317.
Ragland KW, Bryden KM. Combustion engineering. 2nd ed. Boca Raton (FL): CRC Press; 2011.
Ragland KW, Aerts DJ, Baker AJ. Properties of wood for combustion analysis. Bioresour Technol 1991;37:161–8.
Ravi MR, Kohli S, Ray A. Use of CFD simulation as a design tool for biomass stoves. Energy Sustain Dev 2002;6(2):20–7.
Ravi MR, Sinha S, Jhalani A, Ray A. Development of a semi-empirical model for pyrolysis of an annular sawdust bed. J Anal Appl Pyrolysis 2004;71:353–74.
Rehfuess E. Fuel for life: household energy and health. Geneva: World Health Organization; 2006.
Schlunder EU, Gnielinski V. Wärme- und stoffübertragung zwischen gut und aufprallendem düsenstrahl. Chem-Ing-Tech 1967;39:578–84.
Schutte E, Prasad KK, Moerman E. Wood combustion studies, part II. Eindhoven, The Netherlands: The Woodburning Stove Group, Eindhoven University of Technology; 1991.
Seban RA, Black LH. Velocity and temperature profiles in a wall jet. Int J Heat Mass Transf 1961;3:255–65.
Shah R, Date AW. Steady-state thermochemical model of a wood-burning cook-stove. Combust Sci Technol 2011;183(4):321–46.
Shah RK, London AL. Laminar flow forced convection in ducts. New York: Academic Press; 1978.
Simmons G, Lee WH. Kinetics of gas formation from cellulose and wood pyrolysis. In: Overend RP, Milne TA, Mudge LK, editors. Fundamentals of thermo-chemical biomass conversion. Amsterdam: Elsevier; 1985.
Steward FR. Prediction of the height of turbulent diffusion buoyant flame. Combust Sci Technol 1970;2:203–12.
Tillman DA, Rosi AJ, Kitto WD. Wood combustion: principles, processes and economics. New York: Academic Press; 1981.
Tinney ER. The combustion of wooden dowels in heated air. 10th Symp (Intl) Comb; 1965. p. 925–30.
Trinks W, Mawhinney MH, Shannon RA, Reed RJ. Industrial furnaces. 4th ed. Hoboken, NJ: John Wiley & Sons; 2003.
Varunkumar S, Rajan NKS, Mukunda HS. Experimental and computational studies on a gasifier based stove. Energ Convers Manag 2012;53:135–41.
Verhaart P. On designing woodstoves. Proc Indian Acad Sci Sect C 1982;5(4):287–326.
Visser P. Unpublished report. Eindhoven, The Netherlands: Eindhoven University, 1984. As cited in [18].
Weerasinghe WMSR, Kumara UDL. CFD approach for modelling of combustion in a semi-enclosed cooking stove. Bangladesh: Proc ICME; 2003.
Wohlgemuth A, Mazumder S, Andreatta D. Computational heat transfer analysis of the effect of skirts on the performance of third-world cookstoves. J Therm Sci Eng Appl 2010;1, 041001-1-10.
World Health Organization (WHO). Addressing the links between indoor air pollution, household energy, and human health; 2002 [WHO/HDE/HID/02.10.].